Materials Today Communications 6 (2016) 81–91

Contents lists available at ScienceDirect

Materials Today Communications

journal homepage: www.elsevier.com/locate/mtcomm

On the strategies for incorporating nanosilica aqueous dispersion in the synthesis of waterborne polyurethane/silica nanocomposites: Effects on morphology and properties

Pablo J. Peruzzo[a,*], Pablo S. Anbinder[b], Francisco M. Pardini[c], Oscar R. Pardini[a,c], Tomas S. Plivelic[d], Javier I. Amalvy[a,c]

[a] Instituto de Investigaciones Fisicoquímicas Teóricas y Aplicadas (INIFTA: UNLP—CONICET CCT La Plata), Universidad Nacional de La Plata, Diag. 113 y 64CC 16 Suc. 4, B1904DPI La Plata, Argentina
[b] Instituto de Física de Materiales Tandil (IFIMAT), CIFICEN, Consejo Nacional de Investigaciones Científicas y Técnicas (CONICET) y Universidad del Centro de la Provincia de Buenos Aires, Pinto 399, B7000GHG Tandil, Argentina
[c] Centro de Investigación y Desarrollo en Tecnología de Pinturas (CIDEPINT: CICPBA—CONICET CCT La Plata), Av. 52 e/121 y 122. B1900AYB La Plata, Argentina
[d] MAX IV Laboratory, Lund University, P.O. Box 118, 221 00 Lund, Sweden

ARTICLE INFO

Article history:
Received 22 January 2016
Accepted 27 January 2016
Available online 9 February 2016

Keywords:
Nanocomposites
Polyurethane/nanosilica
Waterborne dispersions

ABSTRACT

In this work the synthesis of waterborne polyurethane/nanosilica nanocomposites by using two different strategies is presented, starting from a vinyl terminated polyurethane prepolymer (PUP) based on isophorone diisocyanate and polypropylene glycol, and varying the nanosilica content. In one case, the PUP was dispersed in an aqueous solution containing glycerol-functionalized colloidal nanosilica particles and the dispersion was further polymerized; in the other case, the PUP was dispersed in an aqueous media, then colloidal nanosilica was added to the dispersion and then polymerized. A physical mixture was also prepared for comparative purpose. Films were prepared by casting of the aqueous dispersion. The morphology of the dispersions and films depended on the incorporation route of nanoparticles as was observed by SAXS, SEM and TEM. While the blends had significantly less hydrogen bonding between the hard segments of the PU and nanosilica particles, samples prepared by the two different methods proposed in this work showed an strong interaction between both materials in agreement with FTIR and DSC results. Synthesis pathway plays an important role in order to obtain high performance waterborne polyurethane/nanosilica composites, since final properties of the films also depended on the nanoparticle incorporation strategy.

1. Introduction

Organic/inorganic composite materials have been extensively studied for a long time. When inorganic phases in organic/inorganic composites become nanosized, they are called nanocomposites. In polymer nanocomposites the polymer chains are confined to nanoscale dimensions (1–10 nm). These materials have unusual properties which cannot be obtained simply by co-mixing the polymeric component with the inorganic phase at the macroscopic level [1–4]. However, the properties of nanocomposites strongly depend on the organic matrix, inorganic nanofiller and the way in which they are prepared [5–7].

Polyurethane/silica (PU/silica) nanocomposites is one of the combinations that have attracted substantial academic and industrial interest in the last 20 years. In fact, among the numerous organic/inorganic nanocomposites, PU/silica nanocomposites have received much attention in recent years and they have been employed in a variety of applications [8,9]. The incorporation of nanosilica to the polyurethane matrix provide films with improved properties like increased indentation hardness, high resistance to whitening and high permeability to water vapor [10]. These materials are useful also as tough, abrasion-resistant coatings with increasing friction coefficient and reduced tackiness, with no change in gloss [11].

According to the starting materials and processing techniques PU/silica nanocomposites are prepared by three general methods

* Corresponding author. Tel.: +54 221 4257291/7434 (int: 115); fax: +54 221 4254642.
E-mail address: pjperuzzo@inifta.unlp.edu.ar (P.J. Peruzzo).

http://dx.doi.org/10.1016/j.mtcomm.2016.01.002
2352-4928/

[12]: blending [13], sol–gel processes [14,15], and *in situ* polymerization [16,17]. Frontal polymerization was also been used as an alternative way of preparation of these composites [18]. Although considerable efforts have been devoted to the design and controlled fabrication of polymer/silica colloidal nanocomposite particles with tailored morphologies in recent years [19–21], there have not been many reports in the published literature about the preparation and properties of waterborne PU/silica (WPU/silica) nanocomposite materials. Water dispersions are non-toxic, non-flammable, and do not pollute the air, thus rendering these systems safe regarding the environment and they will have great potential applications in the future. With this idea in mind, plenty of work has been done in order to produce these nanocomposites dispersed in aqueous media [22–25]. However, most of these WPU/silica nanocomposites were prepared using organic solvents or by mixing the polyol with silica powder and then reacting with diisocyanate. Moreover, there have been few attempts to used colloidal nanosilica for WPU/silica nanocomposites preparation. Using monodispersed colloidal silica instead of nanosilica powders, or preparing silica network form alkoxysilanes, allow controlling the size distribution of the inorganic component in the hybrid materials, which may be very important for specific optical applications. Grillet et al. [13] prepared nanocomposite materials by drying a mixed colloidal suspension of film-forming latex and silica and Yang et al. [26] prepared WPU/silica hybrids by adding colloidal silica to a waterborne polyurethane. However, these processes seem to be similar to those used for the preparation of a mixture between nanosilica and polyurethane aqueous dispersions. Indeed, these products have been manly formulated from aqueous silica sols with fully hydroxylated surfaces. It has been claimed that surface-modification of the nanosilica by a condensation reaction between the surface silanol groups and alkyloxysilane reagents can enhance colloidal stability [27]. It was also claimed that the existence of functionalized silica improved thermo-stability, hardness and water resistance of composite films effectively and the composite films possessed good transparency [28–30]. This strategy improves the compatibility silica/polymer and achieves a good dispersion of the inorganic filler in the polymer matrix. In addition, these organic surface modifiers can act just as organic compatibilizers or they can bear on one end a functional reactive group (monomer or initiator molecule) that can participate in the polymerization process. In this way, Zhang et al. [28] published the preparation of UV-curable polyester-based waterborne polyurethane/functionalized silica nanocomposites. They employed functionalized silica containing a large number of C=C double bonds which can participate in UV-initiated radical polymerization. Recently Chiacchiarelli et al. [31] report the relationship between nanosilica dispersion degree and the tensile properties of polyurethane nanocomposite. Depending on the silica type and weight concentration, polyol OH numbers, mixing methods and nanosilica surface properties, the final dispersion and the mechanical properties change considerably. They found that using ultrasonic dispersion, high shear mixing or tip sonication have relative effect on the reduction of agglomerate size and the interparticle distance. Bearing this in mind we propose to use functionalized colloidal nanosilica dispersion as starting material for the preparation of polyurethane nanocomposites and different addition strategies of a preformed polyurethane prepolymer. To the authors knowledge no work for synthesis of WPU/nanosilica composites was reported using aqueous colloidal functionalized nanosilica particles. So, in this work we present the synthesis of WPU/nanosilica composites prepared by using two incorporation methods of functionalized nanosilica particles in aqueous dispersion during the WPU synthesis, avoiding the typical drying step of the colloidal nanosilica when this is used as starting material. To avoid polymer particle aggregation we take advantage of the Pickering emulsion capacity of silica nanoparticles [32]. As we used glycerol-functionalized silica nanoparticles aqueous dispersion, and depending on the preparation route, a chemical reaction between the glycerol and isocyanate groups is also possible, giving in this way a chemical bond. The objective of this study is to investigate how the incorporation route of the nanosilica dispersion influences the distribution of the nanoparticles and the properties of PU/nanosilica composite films. A simple physical mixture from the PU dispersion with the colloidal nanosilica was also prepared for comparative purpose. Films prepared from dispersions were characterized by FTIR, TEM, SEM and SAXS. UV–vis, hardness and thermal properties results are also presented and discussed.

Table 1
Recipe for the synthesis of PU prepolymer.

Compound	Weight (g)	Moles
IPDI	100.00	0.45
PPG1000	136.32	0.14
DMPA	13.71	0.10
HEMA	11.71	0.09
DBTDL	0.39	

2. Experimental

2.1. Reagents

Isophorone diisocyanate (IPDI, Aldrich), 2-hydroxy ethylmethacrylate (HEMA, Aldrich), potassium persulfate (KPS, Anedra), hydrazine monohydrate (HZN, Aldrich), dibutyltindilaurate (DBTDL, Aldrich), triethylamine (TEA, U.V.E.) and dimethylol propionic acid (DMPA, Aldrich) were of analytical grade and were used as received. Polypropylene glycol 1000 (PPG1000 Voranol 2110, Dow) was dried and degassed at 80 °C at 1–2 mm Hg before used. Bindzil® CC40 was donated by Eka Chemicals. It is a water-based epoxy silane modified colloidal silica dispersion (glycerol-functionalized silica sol) containing 1–2 attached glycerol groups per nm^2 of silica surface, corresponding to 800 glycerol groups per silica particle, and with a solid content of 40 wt.% [33]. The mean diameter of the Bindzil® CC40 silica sol determined from TEM was 20 ± 4 nm, in agreement with Lee et al.[33].

2.2. Polymer dispersions synthesis

2.2.1. Synthesis of polyurethane prepolymer dispersion (PUP)

The reaction was carried out in a 1000 mL glass jacketed reactor fitted with a reflux condenser, sampling device, N_2 inlet, a feeding inlet, thermocouple and a stainless steel anchor mechanical stirrer. PPG1000 and DMPA were charged into the dried flask. While stirring, the mixture was heated to 98 °C and homogenized and bubbled dried air for approximately 30 min, followed by lowering the temperature to 90 °C and addition of a mixture of IPDI and DBTDL catalyst. The mixture was allowed to continue at this temperature for 2 h. The prepolymer was cooled to 45 °C and HEMA dissolved in acetone was added slowly and allowed to react for approximately 90 min. Then, the temperature was raised to 60 °C and kept constant until the isocyanate (NCO) content reached the desired value (approximately for 90 min). Upon obtaining the theoretical NCO value (ca. 4.7%) the mixture was cooled to 55 °C and TEA (in acetone) was fed in slowly over 50 min. After neutralization the temperature was lowered to room temperature [34]. A typical base formulation of PUP used in this paper is given in Table 1 and a scheme of the synthesis is showed in Fig. 1.

2.2.2. Synthesis of nanosilica/polyurethane dispersions

Two different synthetic methods starting from PU prepolymer (PUP) were used. In one case PUP was dispersed in water containing

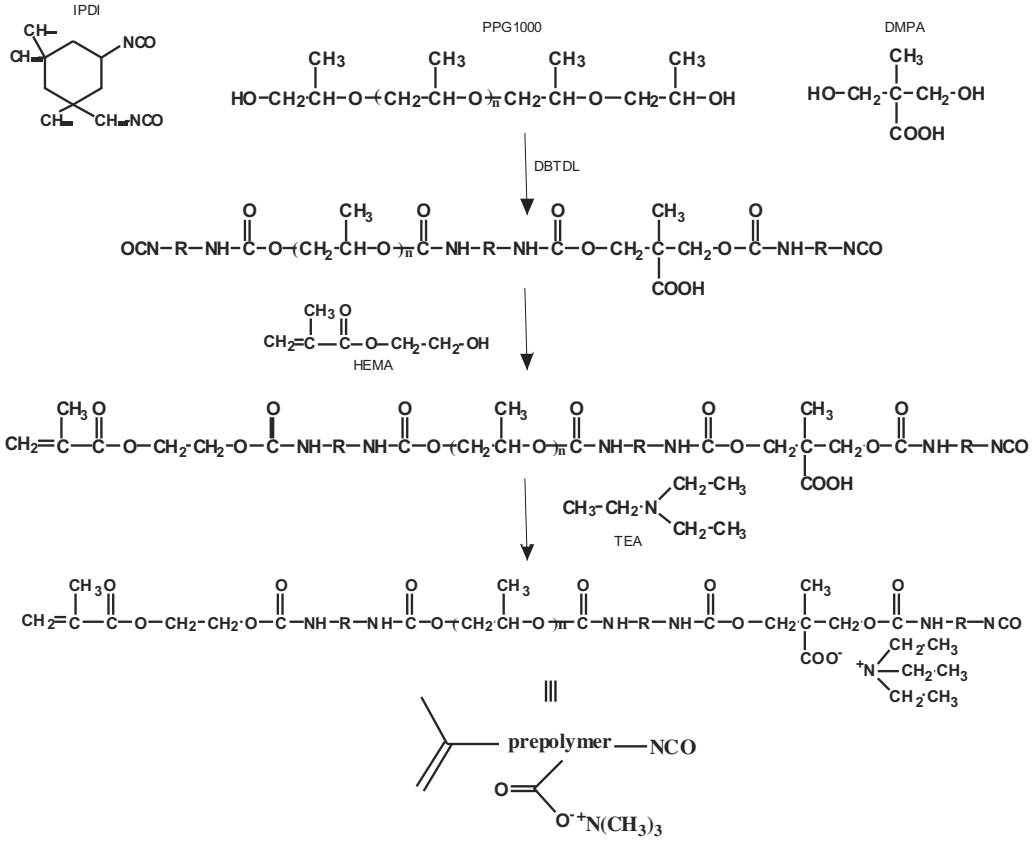

Fig. 1. Schematic synthesis of polyurethanic prepolymer PUP.

the appropriate amount of HZN and the colloidal nanosilica particles. The dispersion was performed at 300 rpm in a glass jacketed reactor at 30 °C during 45 min. Then, the obtained dispersion was subjected to a dispersion polymerization, by adding KPS (0.15 wt.% respect to HEMA content) at 60 °C to obtain an aqueous dispersion of PUP dispersed in a nanosilica dispersion with a posterior polimerization (PU-S)Dp. In the other case, the PUP was dispersed in water containing the appropriate amount of HZN to perform the chain extension reaction in the same conditions of previous system. Then colloidal nanosilica was added drop by drop to the polyurethane dispersion and mixed during 45 min at 100 rpm. The obtained dispersion was polymerized by added KPS (0.15% respect to HEMA content) at 60 °C. The product was an aqueous dispersion of PUD containing nanosilica particles with a posterior polimerization (PUD-S)p (see Fig. 2).

2.2.3. Preparation of nanosilica/polyurethane dispersion mixture

An aqueous dispersion of PU was obtained by adding the PUP to water containing the appropriate amount of HZM to perform the chain extension reaction. The dispersion was performed at about 300 rpm in a glass reactor at 30 °C during 45 min. The aqueous polyurethane dispersion containing vinyl end groups (PUD) was polymerized by adding KPS (0.15% respect HEMA content) at 60 °C, to obtain a PU polymerized dispersion (PUDp). A mixture from the PUDp with the nanosilica (PUDp-S) was prepared for comparative purpose, by adding drop by drop the nanosilica dispersion and mixing during 45 min at 100 rpm. Table 2 presents the samples prepared in this work.

2.3. Film formation

All products prepared from the different strategies were stable dispersions with solid content of about 30 wt.%. Films were prepared by casting the dispersions on a Teflon® substrate by evaporating the water at 30 °C during 48 h.

2.4. Characterization

Fourier-transformed infrared spectroscopy (FTIR) studies were performed using a FT-IR Nicolet 380 spectrometer (Thermo Fisher Scientific, USA) in the ATR mode. The number of scans per experiment was 64. Transmission electron microscopy (TEM) studies were performed using a JEM 1200 EX II—JEOL instrument (Jeol, Japan). Dilute dispersions were dried onto copper grids covered with Formvar™. Scanning electron microscopy (SEM) of the cryo-fractured surfaces of the polyurethane/silica composites were performed using a FEI-Quanta 200 (Netherlands) microscope in both high and low vacuum modes. For Hi-Vac mode, samples were coated using aurum sputtering before the observation, using the secondary electron detector. In Lo-Vac mode, uncoated samples were observed with the back-scattered electron detector (GAD-BSED). Small angle X-ray scattering (SAXS) measurements of dispersions and films were performed at the D02A-SAXS2 beamline at the LNLS (Campinas, Brazil). A monochromatic beam of wavelength 1.608 Å was used and the exposure time was 300 s and 600 s for dispersions and films, respectively. The scattering intensity was registered using a 2D-CCD detector using a sample-detector distance of 2043.72 mm for values of scattering vector

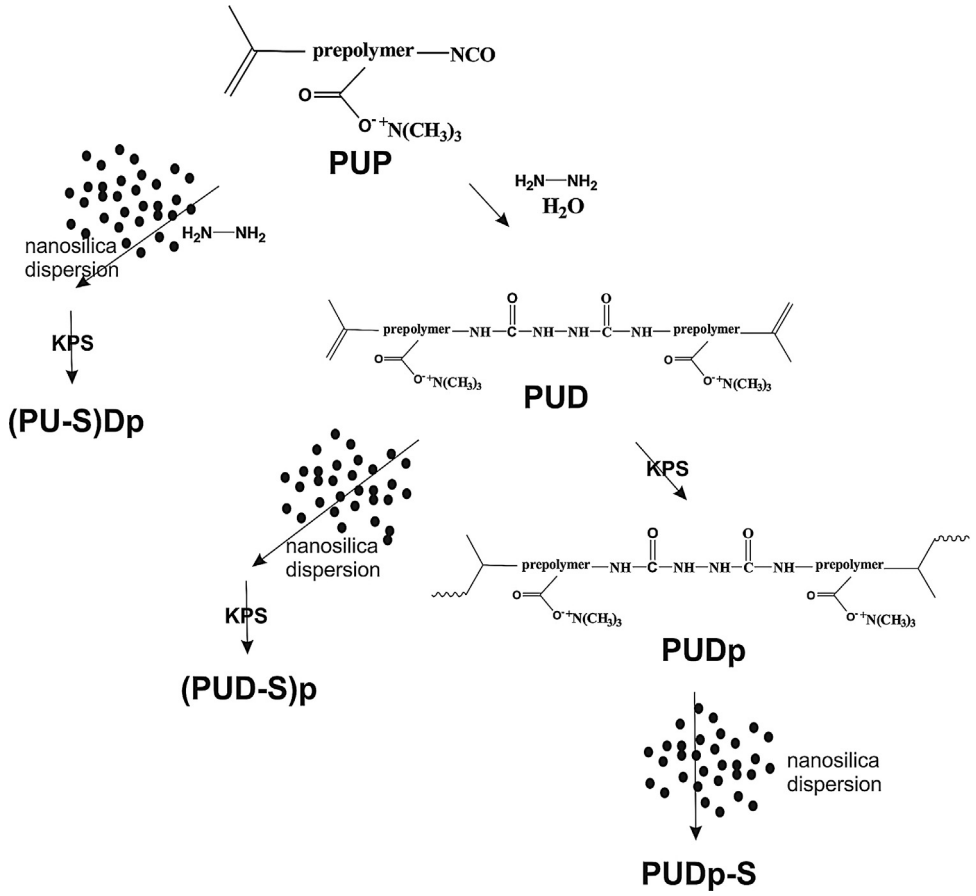

Fig. 2. Schematic synthesis of polyurethane/nanosilica composite dispersions.

Table 2
Composition of polyurethane/nanosilica composites.

Sample name	Nanosilica content (wt. %)	Nanosilica dispersion[a] (g)	PUP (g)	PUD dispersion[b] (g)	PUDp dispersion[b] (g)
(PU-S)Dp 5	5	9.37	71.25	–	–
(PU-S)Dp 10	10	18.75	67.50	–	–
(PU-S)Dp 15	15	28.12	63.75	–	–
(PUD-S)p 5	5	9.37	–	237.50	–
(PUD-S)p 10	10	18.75	–	225,00	–
(PUD-S)p 15	15	28.12	–	212.50	–
(PUDp-S) 5	5	9.37	–	–	237.50
(PUDp-S) 10	10	18.75	–	–	225,00
(PUDp-S) 15	15	28.12	–	–	212.50

[a] 40 wt.% aqueous dispersion.
[b] 30 wt.% aqueous dispersion.

$0.006 < q < 0.013$ Å^{-1} ($q = (4\pi/\lambda)\ \sin(\theta/2)$; θ: scattering angle; λ: wavelength). Acquired data were corrected subtracting the background contribution of the empty cell. One dimensional curves were obtained by integration of the 2D data using the program FIT2D. DSC were performed using a Shimadzu DSC-60 instrument, between −100 °C and +150 °C, at a heating rate of 10 °C min^{-1}. Samples were first heat at 150 °C at 30 °C min^{-1} and cool down at 30 °C min^{-1} before scanning to erase thermal history. A nitrogen gas purge was applied and second heating curves were used for analysis. The thermogravimetric analyses (TGA) were carried out by using a Shimadzu DTA-60 instrument at a heating rate of 10 °C min^{-1} in a nitrogen atmosphere, from room temperature to 600 °C. The UV–vis spectra of films (0.250 mm thickness) were measured using a Genesys 10S UV–vis spectrometer (Thermo Scientific, USA) in a wavelength range from 200 to 800 nm. Tensile properties (such as tensile strength, elongation at break and tension at break) of films were measured at 25 °C using an EMIC DL-3000 (EMIC Ltda., San Pablo, Brazil) tensile-testing machine. Dog-bone-type specimens of 0.250 mm thickness, 6 mm width and 33 mm length were prepared according to the test procedure given in ASTM D-638 (type IV specimen), and a testing speed of 50 mm min^{-1} was used. Buchholz hardness of the composite films were determined according to DIN 53153 with a Buchholz indentation hardness tester (Erichsen, Germany; mass of metal block: 1000 ± 5 g, time of measurements: 30 s). Results are expressed as Buchholz indentation resistance.

3. Results and discussion

3.1. FTIR results

Fig. 3a shows the FTIR spectra of polymerized polyurethane (PUDp) and composites obtained from the different ways and containing 10 wt.% of silica nanoparticles.

The PUDp spectrum shows the typical bands at around 3444 cm^{-1} and 3332 cm^{-1} arising from H—bonded N—H and free N—H stretching vibrations, respectively. Additional observations include an absorption at 1537 cm^{-1} (Amide II band), a broad band centered at 1709 cm^{-1} (free C=O and H—bonded C=O stretching), a signal centered at 1305 cm^{-1} (combination of NH bending and C—N stretching), another absorption at 1239 cm^{-1} (Amide IV band), and a band at 1110 cm^{-1} (C—O—C stretching vibration of polyetherdiol) [35]. The spectrum of nanosilica (see Supplementary information) presents the bands corresponding to symmetric and antisymmetric vibrations of Si—O—Si located at 802 and 1081 cm^{-1}, respectively. In addition, it shows a band at 3450 cm^{-1} assigned to O—H bonds of the —OH groups of the silanol (—Si—OH) and glycerol-derivative groups (—Si—$(CH_2)_3$—O—CH_2—C(OH)—CH_2(OH)) of functionalized silica sol [33]. The spectra of composites and mixture samples showed progressive changes in some bands mainly in the 1100 and 800 cm^{-1} (Si—O—Si) as nanosilica content increase. (PU-S) Dp and (PUD-S) p spectra were similar, however they showed interesting differences compared with the PUDp-S spectrum.

There are two regions of the FTIR spectra of particular interest for the investigation of phase separation of segmented polyurethanes. The first is the carbonyl stretching region, which contains at least five separate bands and is located between 1620 and 1760 cm^{-1} approximately [36,37]. In the (PU-S)Dp and (PUD-S)p samples, there were a greater contribution of the bonded urea C=O band in the 1675–1625 cm^{-1} region compared with the observed in the (PUDp-S) sample, indicating the presence of strong hydrogen bonding interactions in the first ones (Fig. 3b, bottom). The second area of interest is the N—H stretching region, shown in Fig. 3b (top) [36,37]. In this region, samples prepared from simple mixing of the dispersion showed a higher contribution of N—H free band (ca. 3500 cm^{-1}) and a lower contribution in the intensity of the bonded N—H region (3330–3100 cm^{-1}) respect to the samples (PU-S)Dp and (PUD-S)p. This observation is in agreement with the samples behavior in the carbonyl region, where an increase of the H-bonded band was observed for the (PU-S)Dp and (PUD-S)p samples. Therefore, the presence of nanosilica component changes the hydrogen bonding interaction in PU systems depending on the preparation method. The shift of the N—H and CO bands to a lower wavenumber suggests that the incorporation of nanosilica particles promote the microphase separation between hard and soft segments (HS and SS, respectively) due to the strong interaction between nanoparticles and PU matrix in (PU-S)Dp and (PUD-S)p composites. This observation is consistent with a different nanosilica distribution in the PU/nanosilica system depending on the synthetic way, in agreement with TEM and SAXS results (see below). The FTIR spectra do not show obvious difference in the absorbing bands between (PU-S)Dp and (PUD-S)p samples, this is probably because the chemical interaction between the —OH groups of the silica surface (glycerol-derivative and silanol groups) and —NCO groups of prepolymer could produce urethane (with glycerol groups) or silyl-urethane bonds and their bands appear at similar infrared regions to the urethane–urea bonds signals of the PU [38,39].

3.2. TEM, SEM and LV-SEM results

TEM micrographs show a different distribution of silica particles depending on the preparation method (Fig. 4). In (PU-S)Dp, polyurethane particles appear surrounded by nanosilica particles and most of them are evenly dispersed, although some small aggregates can be observed. Important aggregations of silica nanoparticles are observed in mixtures and in (PUD-S)p samples an intermediate situation was observed.

The pattern observed in the (PU-S)Dp suggest an association of PU particles with the silica nanoparticles. One possibility is that a Pickering stabilization mechanism occurs during the prepolymer dispersion and/or a reaction between the surface glycerol and isocyanate groups. In the aggregation zones, the nanosilica particles do not interact with the polymer but they are associated. This is likely ascribed to the organo-modificated surface of the particles and due to the strong tendency of glycerol groups to form intramolecular H-bonds [40].

SEM images of the fracture surfaces of the composites are compared in Fig. 5. The fracture surface of the (PU-S)Dp samples with 5 and 10 wt.% of nanosilica content appear very smooth and similar to the unfilled matrix (see Supplementary information). It suggests that a low amount of silica nanoparticles homogeneously dispersed into PU matrix and the small size of particles almost does not change the original structure and the fracture behavior of pristine polyurethane. However, by increasing the nanosilica content the fracture surface became rough. It is attributed to the modification of the original structure in PU matrix after adding higher levels of nanosilica particles. This trend could be explained by supposing a homogenous distribution of nanoparticles and an improvement of the filler-matrix interactions in the (PU-S)Dp composites up to 10 wt.% filled samples, and therefore a crack propagation path occurring inside the polyurethane matrix. In other way, the fracture surfaces of the (PUD-S)p and (PUDp-S) series show considerably different fractographic features. Samples with 5 wt.% of nanosilica content showed a smooth pattern with stripes near to the air-face. An attempt to incorporate nanosilica particles produced a much rougher pattern. This suggests the presence of a less homogeneous distribution of the silica nanoparticles in the polymer matrix for these samples.

Fig. 6 shows the Low Vacuum Scanning Electron Microscopy of uncoated samples containing 10 wt.% of nanosilica. They show the same tendency observed in TEM and SEM, i.e. the fracture surface of the (PU-S)Dp is smooth and become rougher in the (PUD-S)p and blend systems. Moreover, nanosilica particles (light dots) are seen homogeneously distributed in the bulk material.

3.3. SAXS results

Fig. 7 shows the SAXS curves for the nanosilica particles, PU and samples with 5 wt.% of nanosilica content (Fig. 7a: dispersions; Fig. 7b: films).

For the dispersions (Fig. 7a), it is possible to observe the signal of the PU sample at q around 0.014 $Å^{-1}$ (black line) and the nanosilica at $q = 0.015$ and 0.062 $Å^{-1}$ (gray line). In the solid samples, is possible to observe the typical signal of the PU film sample ($q = 0.14$ $Å^{-1}$) due to microphase separation between the hard and soft domains composing the polyurethane chains [35,41,42]. For the nanosilica powder (obtained by evaporation of water from the nanosilica dispersion), is possible to observe bumps at $q = 0.038$ and 0.062 $Å^{-1}$. The signal at 0.015 and 0.038 $Å^{-1}$ in the dispersion and solid nanosilica sample, respectively, are related to a nanosilica-nanosilica interference peak and do not necessarily have to appear in the nanocomposites, while the signal at 0.062 $Å^{-1}$ is related to the form factor of the nanosilica particles. For each preparation method, the curves appeared similar between them for the different nanosilica concentrations, except for a scaling factor given by the amount of silica nanoparticles. It is also noteworthy that samples containing 10 and 15 wt.% presented similar curves comparing to the 5 wt.% samples, which is noticeably different in the case of (PU-S)Dp method. SAXS curves of composites showed signals

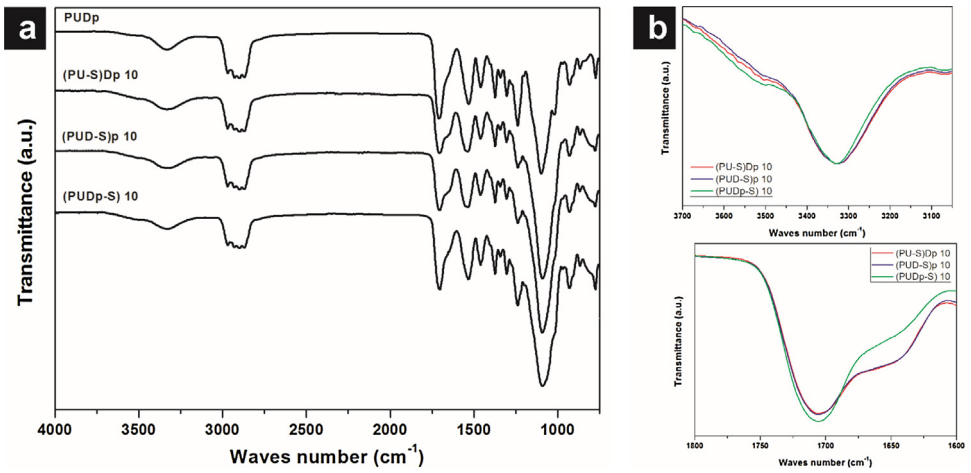

Fig. 3. (a) FTIR spectra of PUDp and PU/nanosilica composites with 10 wt.% nanosilica content; (b) N—H and C=O stretching region of PU/nanosilica composites with 10 wt.% nanosilica content.

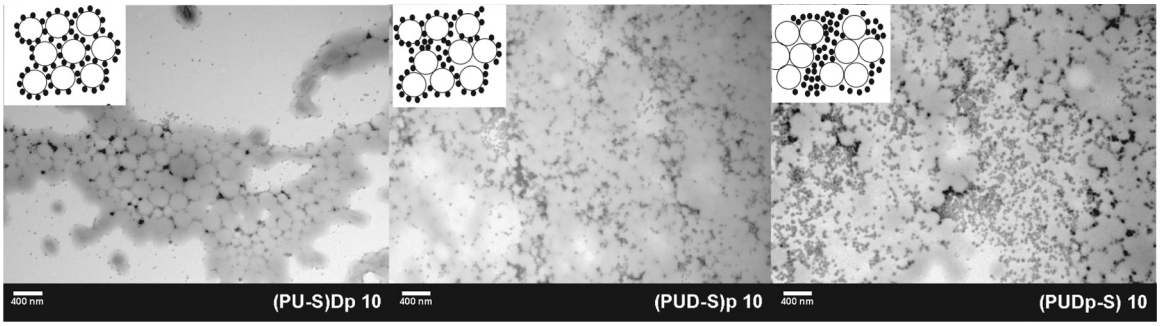

Fig. 4. TEM images of dispersions of PU/nanosilica composites with 10 wt.% of nanosilica content, and schematic representation of the nanosilica distribution in the samples.

related to the contribution of PU and silica particles, but other features were also observed depending on the synthesis method used for their preparation. The curves obtained for (PUD-S)p and (PUDp-S) system appeared very similar between them, but different from the (PU-S)Dp (complete data are available in the Supplementary Information file).

SAXS curves for $q > 0.03$ Å^{-1} do not show appreciable differences for the different strategies. This indicates that the structure is globally similar in all samples, and they have the common features found in rather diluted systems of nanoparticles in a homogeneous matrix. For $q < 0.03$ Å^{-1} some differences appeared in all cases, which can be observed in the curves obtained after the subtraction of the PU contribution, which are presented in Fig. 8.

For the dispersions, (PU-S)Dp and (PUD-S)p samples showed a scattering contribution at q around 0.02–0.03 Å^{-1}, which was not observable in the (PUDp-S) samples. This behavior is related partly to particle interaction, but also to the formation of a different structure depending on the preparation method. This behavior was also observed in the film samples. Consequently, SAXS results demonstrate that the structure of the single particles was maintained during film formation, and this determined the film structure.

Preliminary results from modeling of this systems using a model for raspberry particles [43] could explain the differences observed between samples prepared in this work, which is consistent with a Pickering stabilization mechanism during the prepolymer dispersion in the (PU-S)Dp method, in agreement with TEM results exposed above.

3.4. Comparison of film properties

In this section we are comparing properties of films prepared with the different strategies. Regarding optical properties, all films show high transmittance ($T > 80\%$) in the 400–800 nm region of the UV–vis spectra (see Supplementary information) indicating that the aggregation of nanosilica particles do not affect the transmittance. The DSC curves of the samples prepared in this work are presented in Fig. 8 and thermal data obtained from their are presented in Table 3. Typically, the PUs display multiple DSC transitions related to HSs and SSs [44–48]. In this case, two glass transition points can be observed in the thermograms of the PUDp (Fig. 9). The glass transition observed at around −30 °C was associated with the soft polyether segments of the polymer chain (Tg_s), where the transition observed at around 50 °C reflected the motion onset of the hard segments (Tg_h). As the nanosilica content increased there was an slightly increasing of the Tg_h for the (PU-S)Dp and (PUD-S)p systems respect to PUDp sample. Moreover, an increase of the nanosilica content produced a decrease in the Tg_h value for both systems. This is probably related to the H-bond interaction between the hard segments of the PU polymer and silica nanoparticles, restringing the segmental motion of these domains resulting in an increase of the Tg_h [49,50]. In addition, this interaction produces a higher phase separation between hard segments and soft segments in the PU, in agreement with FTIR results. The last situation results in a higher flexibility of the soft segments producing a decrease of Tg_s values which appeared shifted to the Tg value observed for the PPG1000 polyol (−70 °C). However, blend system

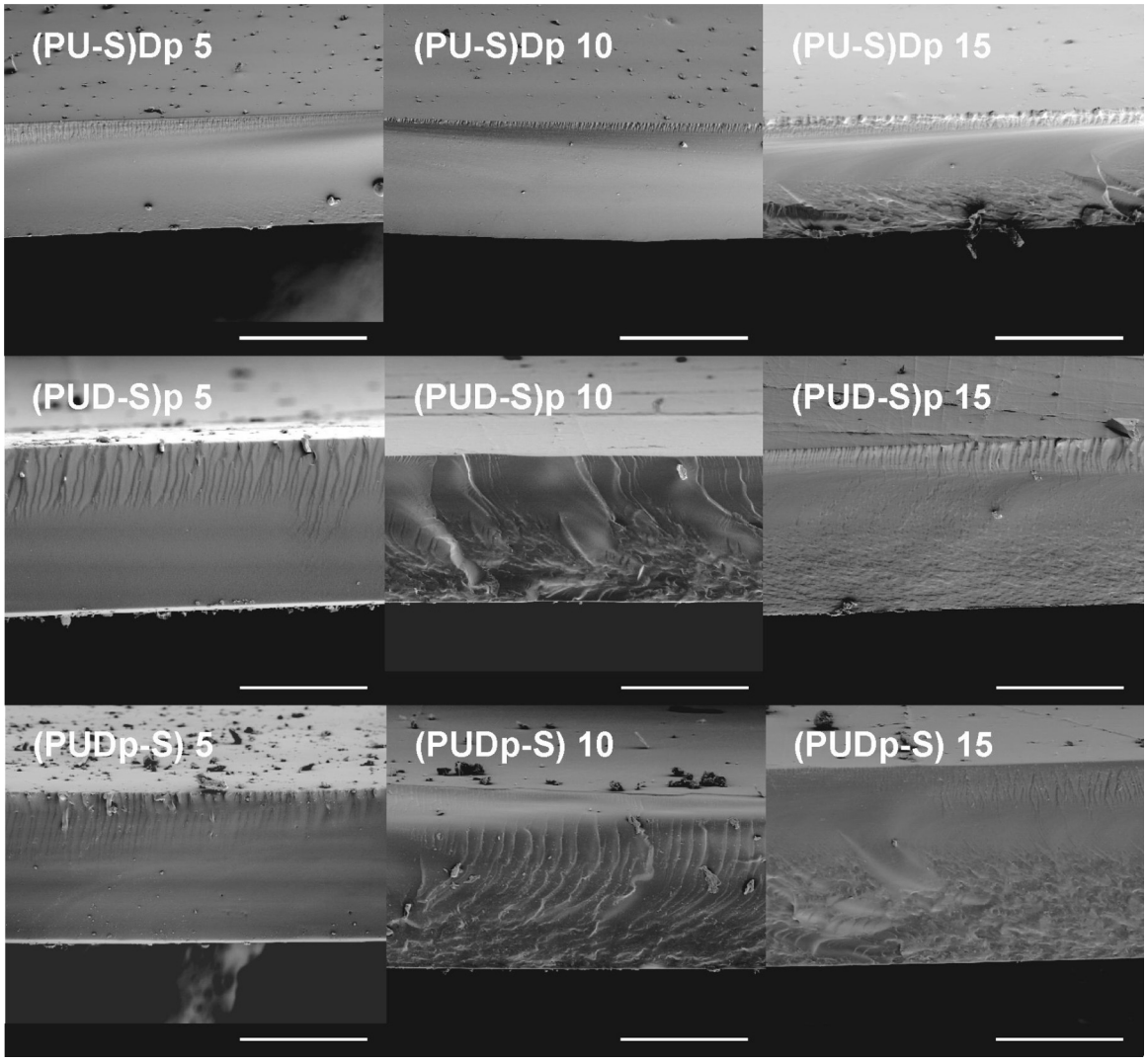

Fig. 5. SEM images of PU/nanosilica composites (scale bar is 200 μm for all micrographs).

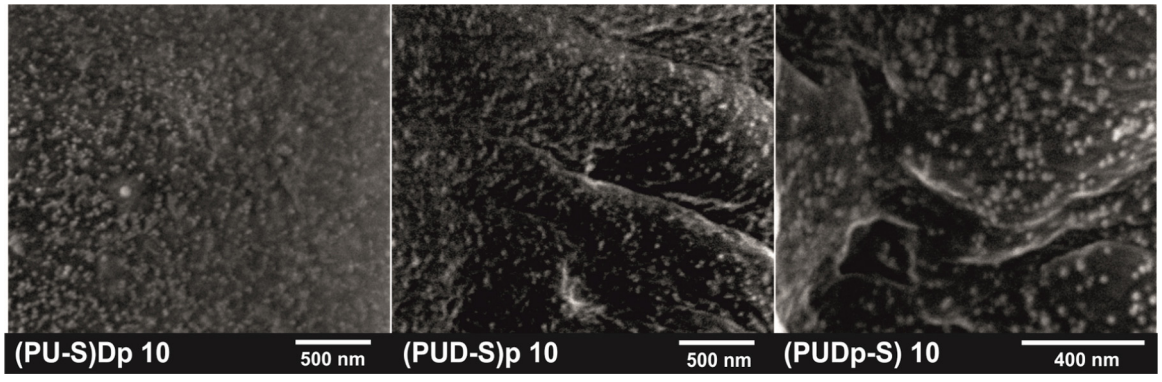

Fig. 6. LV-SEM images of PU/nanosilica composites with 10 wt.% of silica content.

show similar DSCs profiles like PUDp, indicating that the polymeric matrix maintain its general properties as expected for a mixture. In addition, for blended samples an exotherm located at around 80 °C, probably related to a crystallization temperature (Tc) of the HS in the PU matrix, was observed at all nanosilica concentration with an increase of Tc as nanosilica content increases. For samples obtained from the other strategies, this transition is nearly absent at lower nanosilica content, and temperature slightly downshifts with increasing the nanoparticle loading. The DSC results provide strong evidence regarding the nanocomposite phase morphology, and indicate that nanosilica particles are present preferentially in the HS-rich domains. The interaction between nanoparticles and the HS also distorts HS chain conformation in agreement with FTIR results, which hinders crystallization [49].

The maximal decomposition temperature, Td_{max}, calculated from the maximum of the derivative weight loss versus tempera-

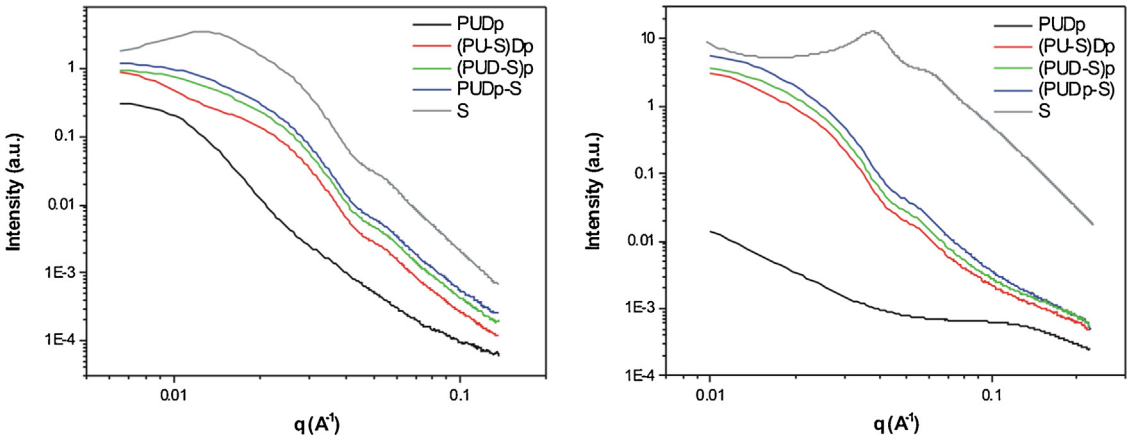

Fig. 7. SAXS curves of PU and PU/nanosilica composites containing 5 wt.% of nanosilica. (a) dispersions, (b) films.

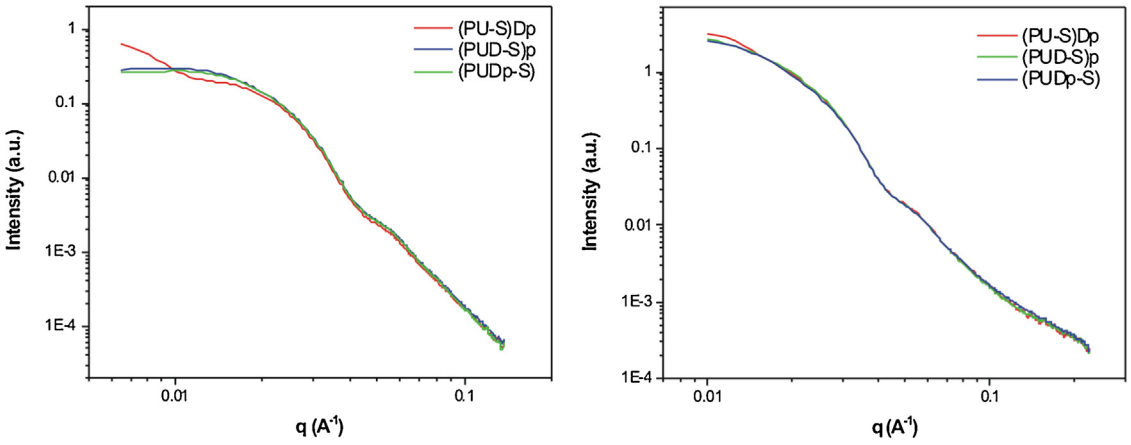

Fig. 8. SAXS curves of PU and PU/nanosilica composites containing 5 wt. % of nanosilica after the substraction of the PU sample contribution. (a) dispersions, (b) films. Curves were overhead at high *q* values.

Table 3
Thermal properties of the samples prepared in this work.

	Glass transition temperatures						Decomposition temperature		
	Tg_s (°C)			Tg_h (°C)			$T_{d,max}$ (°C)		
PUPp	−30			44			360		
Nanosilica content (wt.%)	(PU-S) Dp	(PUD-S) Dp	(PUDp-S)	(PU-S) Dp	(PUD-S) Dp	(PUDp-S)	(PU-S) Dp	(PUD-S) Dp	(PUDp-S)
5	−57	−55	−20	46	47	40	356	345	357
10	−56	−57	−22	45	45	44	351	368	361
15	−55	−57	−22	45	41	45	366	361	364

ture curve from TGA measurements, is also given in Table 3 (the complete thermograms are shown in the Supplementary information file). PUs systems not presents, in general, high thermal stability. In our samples, the thermal degradation begins at about 250 °C and presents a bimodal profile [51]. The thermal indexes T_5 and T_{50}, the decomposition temperatures corresponding to a 5% and 50% weight loss, and Td_{max} indicated a slightly improvement in the thermal stability of the nanocomposites with nanosilica content higher than 10 wt.% compared to the pure polymer, regarding the preparation method. The increase of the decomposition temperature is likely due to the interaction between PU and nanosilica particles. This interaction limits the segmental movement of the polymer chains and, as a consequence, retards the degradation of the materials [25,49]. It can be noticed that the amount of the residue after assay (inset in the TGA graphics showed in Supplementary information file) are in agreement with the theoretical filler amount for the nanocomposites. The slight discrepancies can be attributed to the heterogeneous distribution of silica during film formation, as well as the organic content of the organomodified silica. Mechanical properties of the films (Fig. 10) showed quite different behavior when comparing the materials obtained from the different strategies proposed in this work. When comparing the effect of silica content in each system, physical mixtures presented a gradual change in their parameters as the nanosilica content increase. In contrast, both (PU-S)Dp and (PUD-S)p samples presented a similar behavior between them and completely different to the (PUDp-S) materials, with a non clear trend with increasing silica content. Interesting enough is the fact that mixtures showed higher stress at break and Young's modulus than (PU-S)Dp and (PUD-S)p, which presented higher elongation at break. This characteristic can be attributed to the modification of the polymer during synthesis, avoiding the typical dispersion and chain

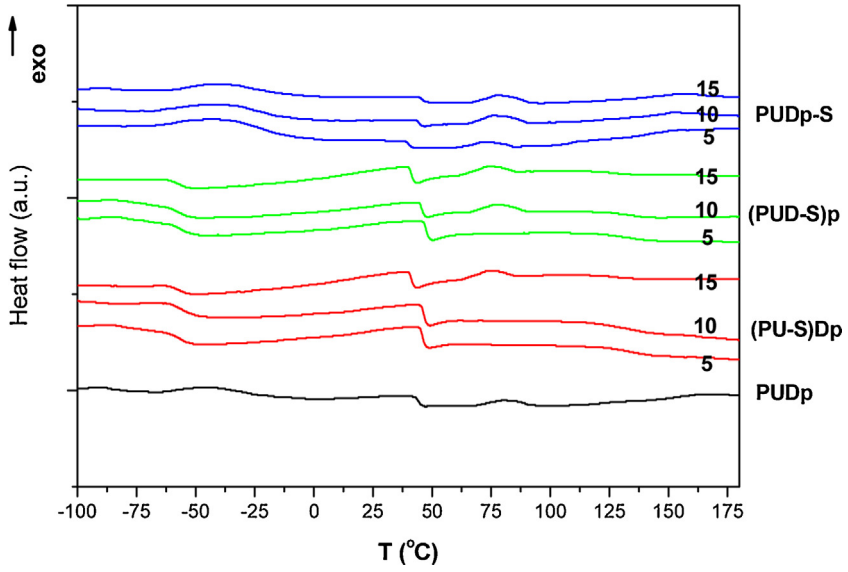

Fig. 9. DSC of PUDp and polyurethane/nanosilica composites.

Table 4
Buchholz hardness values of PUDp and PU/nanosilica composites.

	Buchholz hardness		
PUDp	19		
Nanosilica content (wt.%)	(PU-S)Dp	(PUD-S)p	(PUDp-S)
5	28	24	19
10	30	24	22
15	31	24	20

extension mechanism of the PU when the nanosilica is present in the aqueous media. An increase in elongation without substantially sacrificing material modulus and strain-at-break is significant in (PU-S)Dp and (PUD-S)p samples. This mechanical properties enhancement for *in situ* composites, compared with the blended composites, is a result of the PU-nanosilica interaction and distribution of nanosilica particles within the PU matrix [49,52].

Buchholz hardness of (PU-S)Dp and (PUD-S)p samples (Table 4) showed a similar trends, increasing the value with silica content up to 5 wt.% and keeping constant with the addition of more nanosilica particles. This behavior is quite different from the mixtures which show a constant hardness value, only slightly higher than the pure PU. Buchholz results show that (PU-S)Dp systems are harder than those prepared by simple mixture, whereas (PUD-S)p systems show an intermediate behavior.

The literature is rich with examples that show the changes of mechanical and thermal properties in PU/nanosilica composites, sometimes with opposite results between the works. However, the literature emphasizes also that the filler-polymer interfacial area, filler-polymer matrix compatibility, good dispersion and wettability of the filler within the polymer matrix are responsible for the effects on properties [49,50,52,53]. For this reason, the behavior of the mechanical and thermal properties is controversial because of the inherent complexity of these materials. The understanding of how nanoparticles impact the properties of polymers is still in study. Anyway, the properties obtained for the materials prepared in this work showed that they have a different behavior depending on the way of nanosilica incorporation route, revealing they are different materials from a physical properties point of view, despite the fact that they are formed by the same chemical components.

4. Conclusions

Water-based PU/silica nanocomposites have been synthesized from two different strategies and characterized to investigate the effect of varying the way of nanosilica incorporation on the resulting morphology and film properties. The effect of varying the nanosilica content was also evaluated. Physical mixtures from the polyurethane dispersion and the colloidal nanosilica were also prepared for comparative purpose. The distribution of the silica particles is affected depending on the way of their incorporation during the polyurethane synthesis process. The selected strategy leads to nanocomposites ranging from polymer particles with high coverage of nanosilica particles to physical mixtures with greater amount of silica dispersed in the aqueous medium. The incorporation of nanosilica particles during the synthesis of polyurethane promotes the microphase separation between hard and soft segments in the polymer matrix due to the strong interaction between nanoparticles and PU matrix. As consequence, some properties of films also changed accordingly. Results indicated that synthesis pathway is an important variable in the preparation of nanocomposite polymeric materials, since final morphology and properties of these systems can be tunned by modifying the nanoparticle incorporation strategy during synthesis of colloidal polyurethane/nanosilica composites.

Acknowledgments

This research was partially supported by the LNLS (Brazilian Synchrotron Light Laboratory, Brazil - proposal D11A-SAXS 8775/10). We thank Eka Chemicals AB (Sweden) for donation of Bindzil® colloidal silica samples. We thank CICPBA (Comisión de Investigaciones Científicas de la Provincia de Buenos Aires, Argentina) and ANPCyT (Agencia Nacional de Promoción Científica y Tecnológica, Argentina) for their financial assistance. JIA and ORP are members of CICPBA. PJP, FMP and PSA are members of CONICET.

Appendix A. Supplementary data

Supplementary data associated with this article can be found, in the online version, at http://dx.doi.org/10.1016/j.mtcomm.2016.01.002.

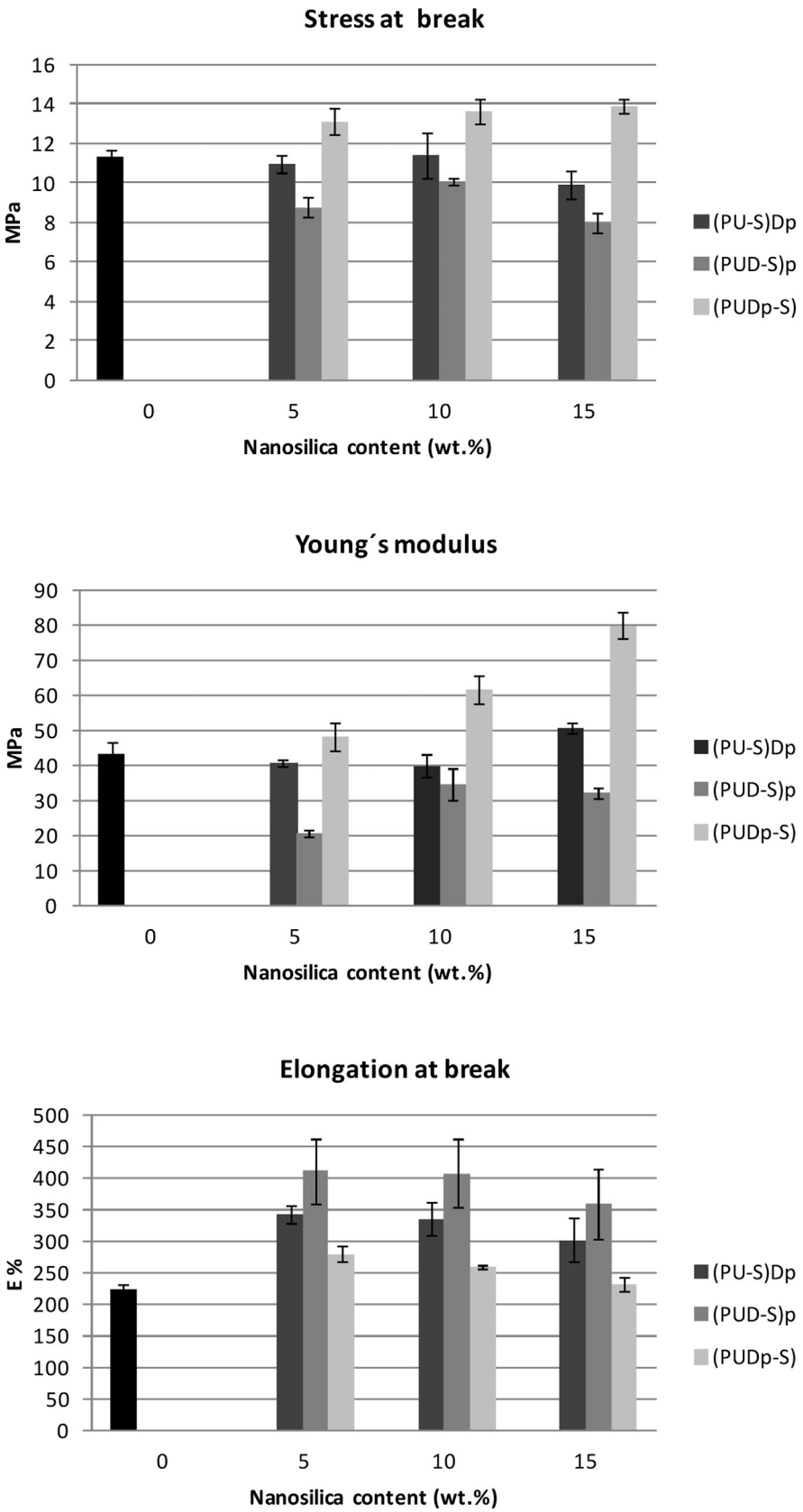

Fig. 10. Mechanical properties of samples prepared in this work.

References

[1] K. Yano, A. Usuki, A. Okada, T. Kurauchi, O. Kamigaito, Synthesis and properties of polyimide-clay hybrid, J. Polym. Sci. A Polym. Chem. 31 (10) (1993) 2493–2498.
[2] Y. Kojima, K. Fukumori, A. Usuki, A. Okada, T. Kurauchi, Gas permeabilities in rubber-clay hybrid, J. Mater. Sci. Lett. 12 (12) (1993) 889–890.
[3] P.B. Messersmith, E.P. Giannelis, Polymer-layered silicate nanocomposites: *in situ* intercalative polymerization of ε-caprolactone in layered silicates, Chem. Mater. 5 (8) (1993) 1064–1066.
[4] P.B. Messersmith, E.P. Giannelis, Synthesis and barrier properties of poly(ε-caprolactone)-layered silicate nanocomposites, J. Polym. Sci. A Polym. Chem. 33 (7) (1995) 1047–1057.
[5] Y.C. Ke, P. Stroeve, Polymer-Layered Silicate and Silica Nanocomposites, Elsevier, Netherlands, 2005.
[6] J.H. Koo, in: P. Kenneth McCombs (Ed.), Polymer Nanocomposites. Processing, Characterization and Applications, McGraw-Hill, USA, 2006.
[7] I.-Y. Jeon, J.-B. Baek, Nanocomposites derived from polymers and inorganic nanoparticles, Materials 3 (6) (2010) 3654–3674.
[8] K. Kusakabe, S. Yoneshige, S. Morooka, Separation of benzene/cyclohexane mixtures using polyurethane-silica hybrid membranes, J. Membr. Sci. 149 (1) (1998) 29–37.
[9] M.A. Bahattab, J. Donate-Robles, V. García-Pacios, J.M. Martín-Martínez, Characterization of polyurethane adhesives containing nanosilicas of different, particle size, Int. J. Adhes. Adhes. 31 (2) (2011) 97–103.
[10] Z. Petrovic, I. Javni, A. Waddon, G. Bánhegyi, Structure and properties of polyurethane–silica nanocomposites, J. Appl. Polym. Sci. 76 (2) (2000) 133–151.
[11] E. Barna, B. Bommer, J. Kürsteiner, A. Vital, O. Trzebiatowski, W. Koch, B. Schmid, T. Graule, Innovative scratch proof nanocomposites for clear coatings, Compos. Part A: Appl. Sci. 36 (4) (2005) 473–480.
[12] H. Zou, S. Wu, J. Shen, Polymer/silica nanocomposites: preparation, characterization, properties, and applications, Chem. Rev. 108 (9) (2008) 3893–3957.
[13] A.-C. Grillet, S. Brunel, Y. Chevalier, S. Usoni, V. Ansanay-Alex, J. Allemand, Control of the morphology of waterborne nanocomposite films, Polym. Int. 53 (5) (2004) 569–575.
[14] H.T. Jeon, M.K. Jang, B.K. Kim, K.H. Kim, Synthesis and characterizations of waterborne polyurethane–silica hybrids using sol–gel process, Colloid Surf. A 302 (1–3) (2007) 559–567.
[15] L. Verdolotti, M. Lavorgna, R. Lamanna, E. Di Maio, S. Iannace, Polyurethane-silica hybrid foam by sol gel approach: chemical and functional properties, Polymer 56 (2015) 20–28.
[16] X. Chen, L. Wu, S. Zhou, B. You, *In situ* polymerization and characterization of polyester-based polyurethane/nano-silica composites, Polym. Int. 52 (6) (2003) 993–998.
[17] X. Chen, B. You, S. Zhou, L. Wu, Surface and interface characterization of polyester-based polyurethane/nano-silica composites, Surf. Interface Anal. 35 (4) (2003) 369–374.
[18] S. Chen, J. Sui, L. Chen, J. Pojman, Polyurethane–nanosilica hybrid nanocomposites synthesized by frontal polymerization, J. Polym. Sci. A Polym. Chem. 43 (8) (2005) 1670–1680.
[19] J.I. Amalvy, M.J. Percy, S.P. Armes, H. Wiese, Synthesis and characterization of novel film-forming vinyl polymer/silica colloidal nanocomposites, Langmuir 17 (16) (2001) 4770–4778.
[20] V. Castelvetro, C. De Vita, Nanostructured hybrid materials from aqueous polymer dispersions, Adv. Colloid Interface 108–109 (2004) 167–185.
[21] J.A. Balmer, O.O. Mykhaylyk, A. Schmid, S.P. Armes, J.P.A. Fairclough, A.J. Ryan, Characterization of polymer-silica nanocomposite particles with core–shell morphologies using Monte Carlo simulations and small angle X-ray scattering, Langmuir 27 (2011) 8075–8089.
[22] B.K. Kim, J.W. Seo, Properties of waterborne polyurethane/nanosilica composite, Macromol. Res. 11 (3) (2003) 198–201.
[23] H. Yu, Q. Yuan, D. Wang, Y. Zhao, Preparation of an ultraviolet-curable water-borne poly(urethane acrylate)/silica dispersion and properties of its hybrid film, J. Appl. Polym. Sci. 94 (4) (2004) 1347–1352.
[24] J.-J. Chen, C.-F. Zhu, H.-T. Deng, Z.-N. Qin, Y.-Q. Bai, Preparation and characterization of the waterborne polyurethane modified with nanosilica, J. Polym. Res. 16 (4) (2009) 375–380.
[25] L. Wang, Y. Shen, X. Lai, Z. Li, Effect of nanosilica content on properties of polyurethane/silica hybrid emulsion and its films, J. Appl. Polym. Sci. 119 (6) (2011) 3521–3530.
[26] C.-H. Yang, F.-J. Liu, Y.-P. Liu, W.-T. Liao, Hybrids of colloidal silica and waterborne polyurethane, J. Colloid Interf. Sci. 302 (1) (2006) 123–132.
[27] P. Greenwood, H. Lagnemo Aqueous silica dispersion. WO2004035474 A8 Patent (2004).
[28] L. Zhang, H. Zhang, J. Guo, Synthesis and properties of UV-curable polyester-based waterborne polyurethane/functionalized silica composites and morphology of their nanostructured films Ind, Eng.Chem. Res. 51 (25) (2012) 8434–8441.
[29] I.A. Rahman, M. Jafarzadeh, C.S. Sipaut, Synthesis of organo-functionalized nanosilica via a co-condensation modification using γ-aminopropyltriethoxysilane (APTES), Ceram. Int. 35 (5) (2009) 1883–1888.
[30] M. Rostami, Z. Ranjbar, M. Mohseni, Investigating the interfacial interaction of different aminosilane treated nano silicas with a polyurethane coating, Appl. Surf. Sci. 257 (3) (2010) 899–904.
[31] L.M. Chiacchiarelli, I. Puri, D. Puglia, J.M. Kenny, L. Torre, The relationship between nanosilica dispersion degree and the tensile properties of polyurethane nanocomposites, Coll. Polym. Sci. 291 (12) (2013) 1–9.
[32] A. Schrade, K. Landfester, U. Ziener, Pickering-type stabilized nanoparticles by heterophase polymerization, Chem. Soc. Rev. 42 (2013) 6823–6839.
[33] D. Lee, J.A. Balmer, A. Schmid, J. Tonnar, S.P. Armes, J.J. Titman, Solid-state nuclear magnetic resonance studies of vinyl polymer/silica colloidal nanocomposite particles, Langmuir 26 (19) (2010) 15592–15598.
[34] O.R. Pardini, J.I. Amalvy, FTIR, ^{1}H-NMR spectra, and thermal characterization of water-based polyurethane/acrylic hybrids, J. Appl. Polym. Sci. 107 (2) (2008) 1207–1214.
[35] P.J. Peruzzo, P.S. Anbinder, O.F. Pardini, J.R. Vega, J.I. Amalvy, Influence of diisocyanate structure on the morphology and properties of waterborne polyurethane-acrylates, Polym. J. 44 (3) (2012) 232–239.
[36] L.-S. Teo, C.-Y. Chen, J.-F. Kuo, Fourier transform infrared spectroscopy study on effects of temperature on hydrogen bonding in amine-containing polyurethanes and poly(urethane-urea), Macromolecules 30 (6) (1997) 1793–1799.
[37] J.T. Garrett, R. Xu, J. Cho, J. Runt, Phase separation of diamine chain-extended poly(urethane) copolymers: FTIR spectroscopy and phase transitions, Polymer 44 (9) (2003) 2711–2719.
[38] D. Sondari, A. Septevani, A. Randy, E. Triwulandari, Polyurethane microcapsule with glycerol as the polyol component for encapsulated self healing agent, Int. J. Adv. Eng. Technol. 2 (6) (2010) 466–471.
[39] M.N. Fernandez Hernandez, E. Ruiz Hitzky, Interaccion de isocianatos con sepiolita, Clay Miner. 14 (4) (1979) 295–305.
[40] E.G. Atovmyan, S.V. Koshchii, T.N. Fedotova, Investigation of hydrogen bonds in alkyl glycerol ethers, J. Appl. Spectrosc. 48 (2) (1998) 202–205.
[41] P.J. Peruzzo, P.S. Anbinder, O.R. Pardini, C.A. Costa, C.A. Leite, F. Galembeck, J.I. Amalvy, Polyurethane/acrylate hybrids: effects of the acrylic content and thermal treatment on the polymer properties, J. Appl. Polym. Sci. 116 (2010) 2694–2705.
[42] J. Bolze, M. Ballauff, T. Rische, D. Rudhardts, J. Meixner, *In situ* structural characterization of semi-crystalline polymer latex particles by small-angle X-ray scattering, Macromol. Chem. Phys. 205 (2) (2004) 165–172.
[43] K. Larson-Smith, A. Jackson, D.C. Pozzo, Small angle scattering model for Pickering emulsions and raspberry particles, J. Colloid. Interf. Sci. 343 (1) (2010) 36–41.
[44] R.G.J.C. Heijkants, R.V. van Calck, T.G. van Tienen, J.H. de Groot, P. Buma, A.J. Pennings, P.H. Veth, A.J. Schouten, Uncatalyzed synthesis, thermal and mechanical properties of polyurethanes based on poly(image-caprolactone) and 1 4-butane diisocyanate with uniform hard segment, Biomaterials 26 (20) (2005) 4219–4228.
[45] S. Mondal, J.L. Hu, Structural characterization and mass transfer properties of nonporous segmented polyurethane membrane: Influence of hydrophilic and carboxylic group, J. Membr. Sci. 274 (1–2) (2006) 219–226.
[46] J.T. Koberstein, A.F. Galambos, Multiple melting in segmented polyurethane block copolymers, Macromolecules 25 (21) (1992) 5618–5624.
[47] H.M. Jeong, S.Y. Lee, B.K. Kim, Shape memory polyurethane containing amorphous reversible phase, J. Mater. Sci. 35 (7) (2000) 1579–1583.
[48] Y. Chamberlin, J.P. Pascault, M. Letoffé, P. Claudy, Model hard segments from diphenyl methane diisocyanate and different chain extenders, and corresponding linear block polyurethanes, J. Polym. Sci. A Polym. Chem. 20 (6) (1982) 1445–1456.
[49] M.A. Hood, C.S. Gold, F.L. Beyer, J.M. Sands, C.Y. Li, Extraordinarily high plastic deformation in polyurethane/silica nanoparticle nanocomposites with low filler concentrations, Polymer 54 (24) (2013) 6510–6515.
[50] Z.S. Petrović, Y.J. Cho, I. Javni, S. Magonov, N. Yerina, D.W. Schaefer, J. Ilavský, A. Waddon, Effect of silica nanoparticles on morphology of segmented polyurethanes, Polymer 45 (12) (2004) 4285–4295.
[51] S.M. Cakic, J.V. Stamenkovic, D.M. Djordjevic, I.S. Ristic, Synthesis and degradation profile of cast films of PPG-DMPA-IPDI aqueous polyurethane dispersions based on selective catalysts, Polym. Degrad. Stab. 94 (11) (2009) 2015–2022.
[52] Y.Q. Rao, J. Munro, S. Ge, E. Garcia-Meitin, PU elastomers comprising spherical nanosilicas: balancing rheology and properties, Polymer 55 (23) (2014) 6076–6084.
[53] O. Malay, O. Oguz, C. Kosak, E. Yilgor, I. Yilgor, Y.Z. Menceloglu, Polyurethaneurea-silica nanocomposites: Preparation and investigation of the structure-property behavior, Polymer 54 (20) (2013) 5310–5320.